Global Analysis of Frequency Stability and Inertia in AC Systems Interconnected Through an HVDC

Atsede G. Endegnanew
Kjetil Uhlen
Department of Electric Power Engineering
NTNU
Trondheim, Norway
atsede.g.endegnanew@ntnu.no

***Abstract*—In this paper, global frequency stability and inertia analysis is performed on a power system consisting of two asynchronous grids connected through a High Voltage Direct Current (HVDC) transmission. Frequency and inertia support providing controllers in the HVDC converters are analyzed with both linear/modal analysis and non-linear dynamic simulations. The analyses focus on dynamics that are in the range of seconds to several minutes in the ac grids. Electromechanical and governor (frequency) modes are studied in detail and interactions between the ac grids are identified. The results show that even though the auxiliary frequency controllers in the HVDC converters improve the frequency stability of the grid that is receiving frequency support, they also reduced the damping of the inter-area mode in the grid: especially when frequency controller with inertia is used. DIgSILENT *PowerFactory* simulation tool was used in the study.**

***Index Terms*--Frequency stability, HVDC, Inertia support, Small signal stability**

I. INTRODUCTION

There are less and less rotating masses connected to ac systems as the extent of penetration of variable renewable generations and High Voltage Direct Current (HVDC) interconnections to other ac grids increase. This has raised concerns regarding the amount of fast frequency control reserves and inertia in a synchronous system; particularly in periods of high power import through HVDC links and/or high generation from power electronics interfaced power sources such as wind and solar generations.

Previous works have shown the possibility of providing frequency containment reserves (FCR) and inertia through HVDC links and MTDC grids [1-7]. Frequency Containment Reserve (FCR) is the operational (primary) reserves activated to contain system frequency after the occurrence of an imbalance [8]. Ref [1-3] discuss how these primary frequency reserves can be shared among non-synchronous AC grids connected through a Multi-Terminal HVDC (MTDC) grid. A decentralized control scheme uses droop controller on the frequency error to modify active power flow at a converter terminal of an MTDC. All ac grids connected to the MTDC grid respond to frequency deviation in one grid. The final steady state frequency of each grid will have some amount frequency error which can be removed by a secondary frequency controller as proposed in [2]. Linear analysis was used in [3] to select controller parameters to guarantee stable performance of the system.

Different methods for providing primary frequency and inertia support to onshore grids from HVDC connected offshore wind farms are presented in [4-6]. Since the offshore wind farm collection grid and the onshore grid are not synchronously connected, auxiliary controllers are introduced to the HVDC to signal onshore frequency deviations to the wind farm grid. The converter onshore changes HVDC dc voltage when frequency changes and the offshore HVDC converter changes offshore grid frequency according to the change in dc voltage. The wind turbine converters' controllers sense change in offshore grid frequency make the turbines reduce or increase (depending on the available power) their power output. Alternatively, [6] proposes communication system to transfer onshore frequency signal to offshore HVDC converter and use the energy stored in dc link capacitors for frequency regulation during communication latency period. Ref [7] presents inertia emulation control strategy that uses the energy stored in DC link capacitors in HVDCs.

The HVDC interconnector between the Netherlands and Great Britain, *BritNed*, is equipped with a frequency droop controller to support frequency in Great Britain [9]. The pilot testing started in 2014 and balancing power of ±100MW is transferred for frequency control on top of the market exchange [10]. The technical and economical investigation of trading primary frequency reserves between Western Denmark and Norway via *Skagerrak* HVDC connections will start in 2016 [11], while there already exists a five years agreement for delivery of ±100 MW secondary control power with a matching 100 MW capacity reservation on the *Skagerrak 4* link [12].

978-1-4673-8463-6/16/$31.00 ©2016 IEEE

In the literature, the technical feasibility of frequency reserve sharing strategies are demonstrated through isolated analysis limited to a single synchronous grid with focus on the frequency of the grid under study. However, in a global system where several asynchronous grids are connected through an HVDC links, frequency reserve sharing will also affect the frequency of on the other synchronous zones, which may or may not experience lack of inertia. Therefore, what is needed is a global analysis that considers the entire system, which includes all asynchronous power systems.

The objective of this paper is to demonstrate, through a case study, how such a global analysis of frequency stability can be performed and which methods that can be used for this purpose. In the study, a power system consisting of two asynchronous grids connected through an HVDC grid is analyzed with both linear/modal analysis and non-linear dynamic simulations. The analysis focused on dynamics that are in the range of seconds to several minutes in both ac grids, i.e. the grid that provides frequency and inertia support and the grid that receives these supports. Electromechanical and governor (frequency) modes are studied in detail and interactions between the ac grids are identified.

II. FREQUENCY REGULATION IN AC SYSTEMS

Power system frequency is dependent on balance between active power generation and load demand. Disconnection of a large load or a generator causes active power imbalance and thus deviation from nominal frequency. The deviation in frequency leads to change in generators' speed causing governors to react. A governor controls generator speed by varying the gate position of a turbine to change the generated active power. When a power system has two or more generators with governors, governors are provided with frequency droop characteristics to ensure stable operation. Frequency droop in generators refers to the percentage change in ac grid frequency to percentage change in power output, and is typically in the range of 4 – 9% [13].

In recent times, the share of power from renewable energy resource based power generation systems, such as wind, solar, small hydro, etc. has increased significantly. As these types of systems do not store primary energy resource, a power system with high penetration of renewable energy resources will have low frequency containment reserve (FCR). In addition, the total inertia in the system will be low as most of these types of generators are either power electronics interfaced or are small generators with small inertia. This makes power systems vulnerable to frequency stability problems.

Frequency stability refers to the ability of a power system to maintain the frequency within a nominal range, following a severe system upset that may or may not result in the system being divided into subsystems [14]. It falls in the category of midterm to long term stability studies, where inter-machine synchronizing power oscillations are damped out, the focus is on slower and longer duration phenomena that accompany large disturbances and result large, sustained mismatches between generation and consumption of active and reactive power [15]. Frequency stability has dynamics ranging from tens of seconds to few minutes.

In the literature, control strategies are proposed for HVDCs to participate in ac frequency regulation; especially those connecting offshore wind farms to onshore grids. This is achieved by changing the power flow in the HVDC based on the change in ac grid frequency. Characteristic times of governors activated by the frequency changes range from seconds to minutes while HVDC converters have a much shorter response time. The next section explains how HVDC converters can provide ac frequency support.

III. VSC CONTROL FOR FREQUENCY STABILITY

Fig. 1. shows typical vector control structure for a Voltage Source Converter (VSC). Independent control of active and reactive power is achieved by influencing the voltage drop over the coupling reactor (represented by R and L) by varying the magnitude and phase of the internal VSC voltage (V_c). Using Park transformation, time variant instantaneous voltage and current (a,b,c) values are converted into a d,q,0 vectors that are constants in a rotating d-q reference frame. More details about VSCs and their control structures can be found in [16].

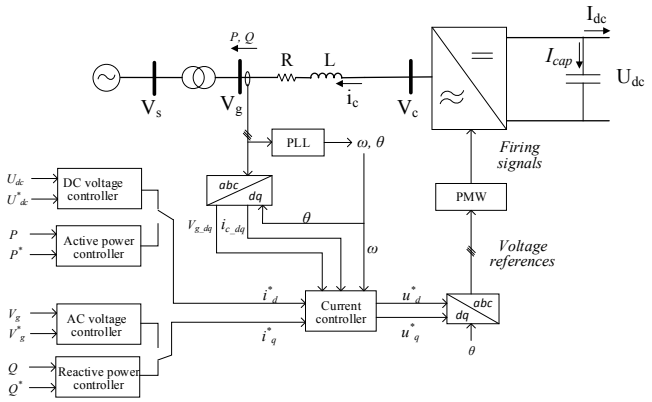

Fig. 1. Control structure for a Voltage Source Converter controller

VSC control is a cascaded control system with inner dq-axis current control loop, and an outer control loop which provides references to the inner loop. The outer loop controls either DC voltage or active power in the d-axis and either reactive power or ac voltage in the q-axis. In HVDCs, the d-axis control of one of the terminals is set to dc voltage control while the other terminal controls active power. When an HVDC participates in ac grid frequency support, the active power control loop is modified to include frequency deviation signal and its control structure becomes as shown in Fig. 2.

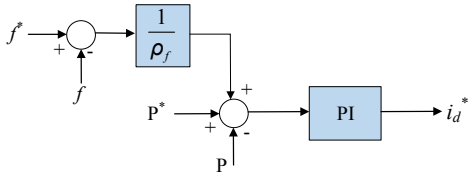

Fig. 2. Control structure for frequency droop controller

where P*, f*, P and f are reference and measured active power and ac grid frequency, respectively. ρ_f is frequency droop of the HVDC and indicates the change in active power flow in

the HVDC for a change in frequency. When ac grid frequency decreases (i.e. the load demand is higher than generated power), the controller increase power flow into the ac grid, and vice versa.

If a derivative controller is used together with a proportional controller, then it would act not only the error between measured and reference frequency values, but also on the rate of change of the error and improves the transient response of the HVDC frequency controller. With this controller, frequency support is also provided during the transient period which is the characteristics of inertia. Here, a phase lead controller is proposed for frequency and inertia support from HVDCs. A phase lead controller is basically a proportional-derivative (PD) controller with a filter and has the form:

$$C(s) = K\left(\frac{1+T_1 s}{1+T_2 s}\right) \tag{1}$$

where $T_1 > T_2$. The controller introduces a positive phase to a system between the corner frequencies $\omega_1=1/T_1$ and $\omega_2=1/T_2$. The maximum amount of phase, ϕ_m, added is at the geometric mean of the two corner frequencies, which is called the center frequency (ω_m). ω_m and ϕ_m are calculated as:

$$\omega_m = \frac{1}{T_2\sqrt{(T_1/T_2)}}$$
$$\sin\phi_m = \frac{(T_1/T_2)-1}{(T_1/T_2)+1} \tag{2}$$

Depending on the value of T_1/T_2, up to 90° phase can be added using a single phase-lead controller. A phase-lead controller improves stability by improving the phase margin of a system. If its parameters are chosen properly, it increases system damping, and decrease rise time and settling time [17].

The block diagram of the modified frequency controller with the phase lead controller is shown in Fig. 3. The controller will improve the transient behavior and stability of ac grid frequency but the steady state behavior of the ac frequency will be the same as the frequency droop controller when $K=1/\rho_f$.

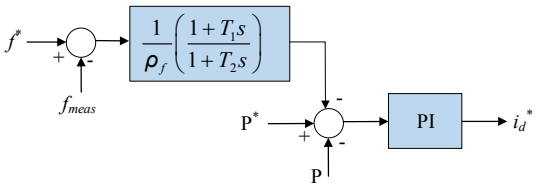

Fig. 3. Frequency controller with inertia support

Global analysis of frequency stability and inertia analysis is performed for a power system with an HVDC that has frequency droop and the proposed phase-lead controllers for frequency control and inertia support. The results are compared and analyzed in the following section.

IV. Simulation Studies And Results

A power system with two asynchronous ac grids interconnected via an 800 MW HVDC link is used for global analysis of frequency stability and inertia. A one line diagram of the study system configuration is presented in Fig. 4. Grid A is a large power system with four generators and long 230 kV transmission lines. It is based on the two area system presented in [15]. Grid B, which is based on a power system presented in [18], is a nine bus power system with three generators and three loads. All generators in the study system have HYGOV and SEXS types of governors and exciters, respectively. In addition, the exciters in Grid A are equipped with STAB1 type of power system stabilizers (PSS) for damping local and inter-area oscillations. DIgSILENT *PowerFactory* was used for the simulation studies, and data for generators, exciters, governors and PSS used in the simulation tool are given in Appendix I.

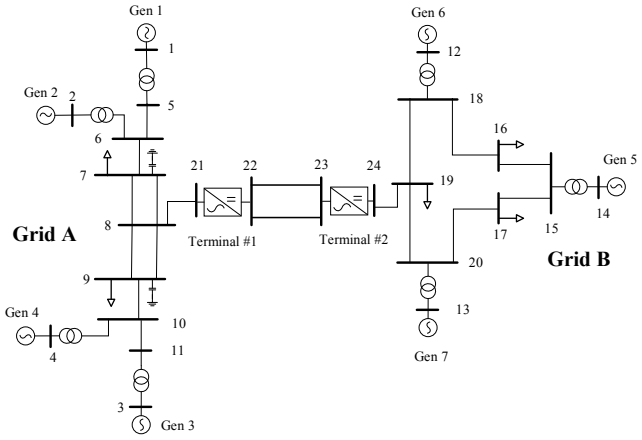

Fig. 4. Study system

The converter controllers at Terminal #1 are operating in DC voltage and reactive power control, while three converter control scenarios are considered for converter controllers at Terminal #2. In the first scenario, Case 1, the converter operates in constant active power control mode and does not participated in frequency control. This case is used as a reference to compare the change in frequency stability and system inertia when the HVDC is involved in frequency control. In the other two scenarios, Case 2 and Case 3, Terminal #2 VSC controllers provide frequency support to Grid B. In Case 2, frequency control with droop (Fig. 2.) is used and in Case 3 both inertia support and frequency support are provided by the VSC-controller (Fig. 3.). In all scenarios, the outer q-axis controller of Terminal #2 is set to reactive power control.

The different cases are studied using linear and time domain analyses. The study evaluates and compares the performance of the controllers, and assesses the electromechanical and frequency stability of both Grid A and B. The initial steady state power flow is 400 MW flowing from Grid A to Grid B. An HVDC frequency droop constant of ρ_f = 20% was used both in Case 2 and 3. ρ_f has a Hz/MW unit and is based on the rating of the converter.

A. Linear analysis

A linear analysis for the study system was carried out for the three different converter control cases at Terminal #2. The

aim of this linear analysis is to investigate how the dynamics of the ac systems are affected when an HVDC is used in ac frequency control to facilitate sharing primary reserves between asynchronous grids. The analysis focused on low frequency electromechanical and governor (frequency) oscillation modes. Electromechanical oscillations are due to oscillations of rotating masses of generators that occur following a disturbance, while frequency oscillations are due to the slow actions of governors following active power imbalance. The electromechanical and governor modes for the studied system were identified from the participation factors of the modes and are listed in TABLE I.

TABLE I. ELECTROMECHANICAL AND GOVERNOR (FREQUENCY) MODES FOR THE THREE CASE STUDIES

Case study	Eigenvalues	f [Hz]	ζ	
Case 1 No HVDC frequency support	-0.23 ± j2.80	0.45	0.08	Electromechanical modes in Grid A
	-0.92 ± j6.37	1.01	0.14	
	-0.91 ± j6.13	0.98	0.15	
	-1.02 ± j10.39	1.65	0.10	Electromechanical modes in Grid B
	-1.32 ± j11.53	1.83	0.11	
	-0.84 ± j2.78	0.44	0.29	
	-0.06 ± j0.16	0.03	0.32	Grid A governor mode
	-0.11 ± j0.40	0.06	0.27	Grid B governor mode
Case 2 HVDC frequency droop support	-0.23 ± j2.80	0.45	0.08	Electromechanical modes in Grid A
	-0.92 ± j6.37	1.01	0.14	
	-0.91 ± j6.13	0.98	0.15	
	-1.02 ± j10.39	1.65	0.10	Electromechanical modes in Grid B
	-1.33 ± j11.53	1.83	0.11	
	-0.75 ± j2.72	0.43	0.26	
	-0.06 ± j0.16	0.03	0.32	Grid A governor mode
	-0.14 ± j0.40	0.06	0.33	Grid B governor mode
Case 3 HVDC frequency and inertia support	-0.23 ± j2.80	0.45	0.08	Electromechanical modes in Grid A
	-0.91 ± j6.37	1.01	0.14	
	-0.91 ± j6.13	0.98	0.15	
	-1.02 ± j10.39	1.65	0.10	Electromechanical modes in Grid B
	-1.34 ± j11.53	1.84	0.12	
	-0.33 ± j2.73	0.43	0.12	
	-0.06 ± j0.16	0.03	0.32	Grid A governor mode
	-0.16 ± j0.41	0.06	0.36	Grid B governor mode

The governor mode of Grid B has 0.06 Hz frequency. The phase-lead controller parameters in Case 3 were selected in such a way that the center frequency for the controller is close to the frequency of this mode. Therefore, T_1 and T_2 were set to 10s and 1s, respectively. This is equivalent to a maximum phase boost of 54.9° at center frequency of 0.32 rad/s (0.05 Hz).

The governor mode in Grid A has damped frequency of 0.03 Hz with 32% damping ratio. Both electromechanical and governor modes in Grid A do not change their position in all three cases of converter controllers implement for the HVDC. They remain unaffected.

The frequency controller is included in controller of Terminal #2, which is the terminal connected to Grid B. Therefore, this grid receives frequency stability and inertia support from Grid A through the HVDC. This is also what is observed from the modal analysis results. The damping ratio of governor (frequency) mode of this grid changes depending on the type of converter control used. When no frequency support was provided, i.e. Case1, the mode had a damping of 27%, while when a frequency droop control was used in Case 2, its damping increased to 32%. In Case 3, where frequency and inertia support is included, the damping ratio for the mode increases further to 36%. The change is only in the real part of the mode and its imaginary part (frequency) does not change. This means that when HVDC is involved in frequency support, the governor mode shifts to the left on the real-imaginary plane improving its damping; as intended.

Even though the frequency control loop in the HVDC improves damping of the frequency mode in Grid B, it also reduces damping of other modes in the grid. One of the electromechanical modes in Grid B (-0.84 ± j2.78), which is an interarea mode between Gen6 and Gen7, became less stable in Case 2 and 3 compared to Case 1. In Case 1, the mode had a damping ratio of 29% while in Case 2 and Case 3, the damping ratio was reduced to 26% and 12%, respectively. The mode shapes of the mode for generator speed state variables reveal that the mode is most observable in Gen 5-7 in Case 1 and Case 2. However, in Case 3, the mode is most observable in Gen 1 and Gen 2 located in Grid A indicating that in Case3 there is an increased dynamic coupling between Grid A and B.

From the modal analysis study, it can be concluded that, the frequency controllers improve the frequency stability of Grid B but reduce the damping of the interarea mode in the grid (especially the frequency controller with inertia support). In addition, in Case 3, there is an increased the dynamic coupling between the two asynchronous grids. The type of frequency controller implemented in the HVDC does not have any effect on the modes in Grid A.

B. Time domain analysis

Two non-linear time domain simulations were run for the three converter control studies. A load disturbance was used to study frequency stability, and short circuit fault in Grid B was used to verify the possible electromechanical interactions identified by the modal analysis.

1) Loss of load in Grid B

A 10% load loss (70 MW) in Grid B at Bus 17 was simulated at t=1s. Immediately after the load loss, the frequency in Grid B is disturbed because of imbalance between generated power and load consumed. Grid A and Grid B frequencies due to the load disturbance for the three converter control scenarios are shown in Fig. 5.

In Case 1, where no frequency control is used in the HVDC, only governors control the grid frequency. Governors' actions are slow because of the large physical time constants of the turbines. It takes 40 seconds until the frequency is stabilized. The maximum frequency in Grid B after the load loss reaches up to 50.5 Hz. When the HVDC is involved in frequency support, then the maximum deviation is reduced and becomes 50.3 Hz and 50.2 Hz in Case 2 and Case 3, respectively. Since the droop constants are the same in both cases, i.e. 20%, the steady state value of the frequency after the disturbance is also the same. It is clear from the low peak and limited rate of change of frequency following the load loss in Case 3 that Grid B receives an inertia support Grid A.

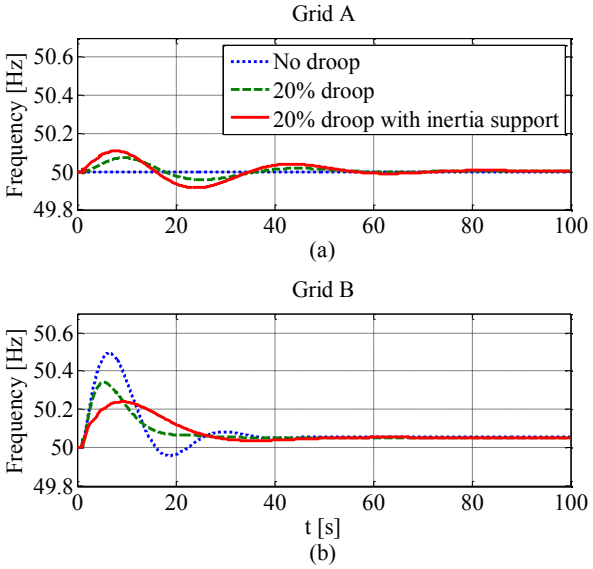

Fig. 5. Frequency responses in (a): Grid A and (b): Grid B

Since the power needed to support Grid B frequency is coming from Grid A, the frequency in latter grid gets disturbed as a result. The disturbance is larger in Case 3 than Case 2 because the power support provided by the grid is larger and faster (see Fig. 6.). Even though the frequency oscillations in Grid A are larger in Case 3 compared to Case 2, the damping of the oscillations are the same for both cases. The type of frequency control applied in Terminal #2 has no adverse effect on the frequency stability of Grid A.

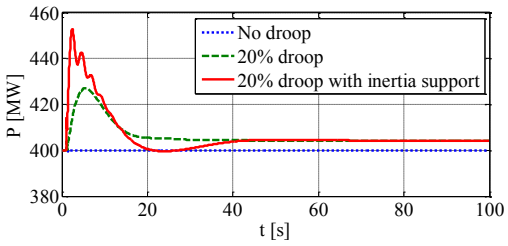

Fig. 6. Active power transferred from Grid A to B through the HVDC

2) Short circuit in Grid B

In order to study specifically the impact the different frequency controllers have on the electromechanical modes, a complete short circuit fault at Bus 18 in Grid B lasting for 100ms was simulated for Case 2 and Case 3. Fig. 7. shows speeds of generators in Grid A (Gen 1-4) and Grid B (Gen 5-7). The generators in Grid B accelerate until the fault is cleared. In Case 2, the electromechanical modes in both grids are highly damped. On the other hand, in Case 3, a poorly damped mode can clearly be seen in Grid B. The frequency of the oscillation of the speed curves (ca. 0.43Hz) is close to the mode that was identified in the modal analysis (-0.33 ± j2.73) to be less stable in Case 3. The mode was also found to have high observability in Gen1 and Gen2 speed state variables. The oscillation frequency of Grid A generators' speed is 0.45 Hz. Since the poorly damped mode in Grid A (-0.23 ± j2.80) also has a similar damped frequency, i.e. 0.45 Hz, it is not possible to point out the contribution of Grid B inter-area mode (-0.33 ± j2.73) in speed oscillations of Grid A generators in Case 3. It is highly likely that the oscillations observed in Grid A in Case 3 are due to higher excitation inter-area mode of the grid caused by the higher power transfer (disturbance) between the two grids. In general, the interaction between the two grids is higher in Case 3.

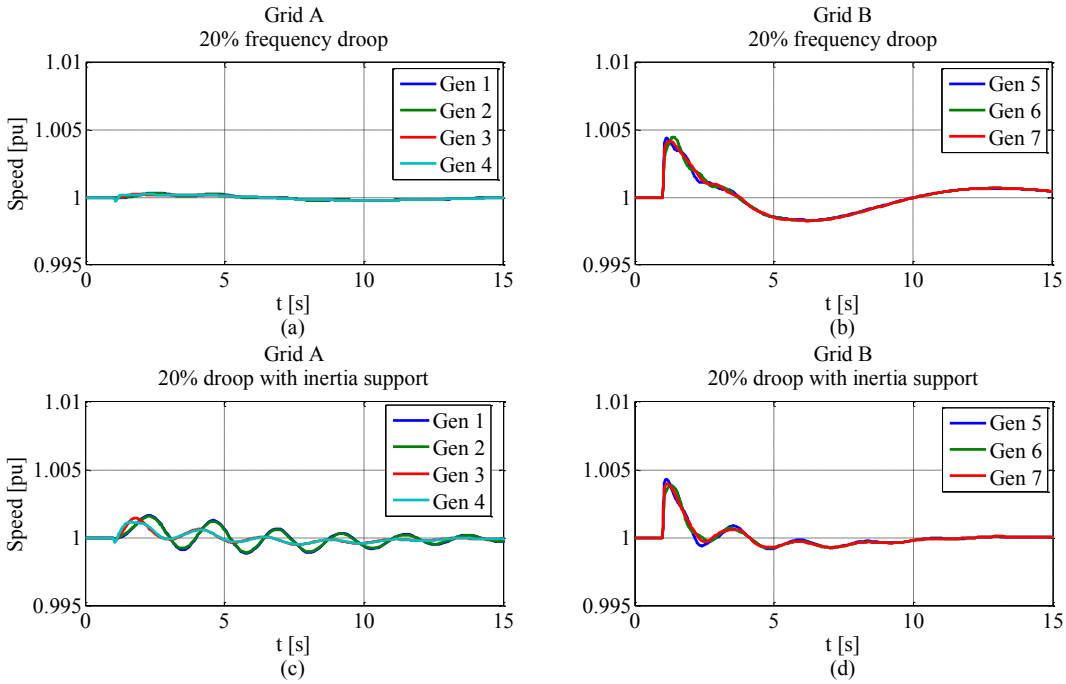

Fig. 7. Frequency responses in Grid A and Grid B for Case 2 ((a) and (b)) and Case 3 ((c) and (d))

V. CONCLUSION

In this paper, global analysis of frequency stability and inertia for two ac systems connected with an HVDC was presented. Modal analysis and non-linear time domain analyses were used in the study. The analyses focused on the dynamic behavior of the ac grids for different types of frequency and inertia support using HVDC converter controllers. It was shown that the frequency controllers perform as expected and improve the frequency stability of the grid receiving the support, and did not have any adverse effect on the grid providing the support. However, the electromechanical stability of the frequency support receiving grid was found to be reduced especially when frequency controller with inertia was used. Furthermore, in the modal analysis identified higher interactions between the two grids. The root cause of these interactions and how proper control design can avoid adverse interactions will be subject for future studies.

APPENDIX I

TABLE II. GENERATOR PARAMETERS

Symbol	Unit	Value		
		Gen 1&2	Gen 3&4	Gen 5-7
MBASE	MVA	900	900	890
V	kV	20	20	20
T'_{do}	s	8	8	5.3
T''_{do}	s	0.03	0.03	0.048
T'_{qo}	s	0.4	0.4	0.62
T''_{qo}	s	0.05	0.05	0.066
H	MW.s/MVA	6.5	6.175	3.9
D	pu	0	0	0
X_d	pu	1.8	1.8	1.72
X_q	pu	1.7	1.7	1.679
X'_d	pu	0.3	0.3	0.488
X'_q	pu	0.55	0.55	0.8
$X''_d = X''_q$	pu	0.25	0.25	0.337
X_l	pu	0.2	0.2	0.266
S(1.0)	–	0.015	0.015	0.0001
S(1.2)	–	9.6	9.6	0.001

TABLE III. GOVERNOR AND TURBINE SETTINGS

Description	Symbol	Gen 1-4	Gen 5-7
Temporary droop	r	0.4	0.5
Gov time constant	Tr	4	5
Filter time const	Tf	0.05	0.05
Servo time const	Tg	0.5	1
Water starting time	Tw	1	1
Turbine gain	At	1.2	1.2
frictional losses factor [pu]	Dturb	0.5	0.5
No load flow	qnl	0.08	0.08
Permanent droop	R	0.05	0.05
Minimum gate limit	Gmin	0	0
Gate velocity limit	Velm	0.167	0.167
Maximum gate limit [pu]	Gmax	1	1

TABLE IV. AVR AND EXCITER SETTINGS

Symbol	Gen 1-4	G5	G6 and G7
Tb	10	10	1
Ta	1	1	1
K	100	100	100
Te	0.05	0.5	0.5
Emin	-3	-3	-3
Emax	3	3	3

TABLE V. PSS SETTINGS

Symbol	K	T_1	T_2	T_3	T_4	T_w	y_{min}	y_{max}
Gen 1-4	5	3.36	0.0337	0	0	3	-0.1	0.1

REFERENCES

[1] T. M. Haileselassie and K. Uhlen, "Primary Frequency Control of Remote Grids Connected by Multi-Terminal Hvdc," in *Power and Energy Society General Meeting, 2010 IEEE*, 2010, pp. 1-6.
[2] D. Jing, Y. Phulpin, A. Sarlette, and D. Ernst, "Voltage Control in an Hvdc System to Share Primary Frequency Reserves between Non-Synchronous Areas," presented at the 17th Power Systems Computation Conference (PSCC-11), Stockholm, 2011.
[3] N. R. Chaudhuri, R. Majumder, and B. Chaudhuri, "System Frequency Support through Multi-Terminal Dc (Mtdc) Grids," *Power Systems, IEEE Transactions on,* vol. 28, pp. 347-356, 2013.
[4] T. M. Haileselassie, R. E. Torres-Olguin, T. K. Vrana, K. Uhlen, and T. Undeland, "Main Grid Frequency Support Strategy for Vsc-Hvdc Connected Wind Farms with Variable Speed Wind Turbines," in *PowerTech, 2011 IEEE Trondheim*, 2011, pp. 1-6.
[5] C. L. Moreira, J. R. Gouveia, and B. Silva, "Participation of Multi-Terminal Hvdc Grids in Frequency Regulation Services," in *Compatibility and Power Electronics (CPE), 2015 9th International Conference on*, 2015, pp. 202-209.
[6] L. Hongzhi and C. Zhe, "Contribution of Vsc-Hvdc to Frequency Regulation of Power Systems with Offshore Wind Generation," *Energy Conversion, IEEE Transactions on,* vol. 30, pp. 918-926, 2015.
[7] Z. Jiebei, C. D. Booth, G. P. Adam, A. J. Roscoe, and C. G. Bright, "Inertia Emulation Control Strategy for Vsc-Hvdc Transmission Systems," *Power Systems, IEEE Transactions on,* vol. 28, pp. 1277-1287, 2013.
[8] (30.11.2015). Available: https://emr.entsoe.eu/glossary/bin/view/ENTSO-E+Common+Glossary/
[9] S. P. Teeuwsen and R. Rossel, "Dynamic Performance of the 1000 Mw Britned Hvdc Interconnector Project," in *Power and Energy Society General Meeting, 2010 IEEE*, 2010, pp. 1-8.
[10] J. E. S. de Haan, C. Escudero Concha, M. Gibescu, J. van Putten, G. L. Doorman, and W. L. Kling, "Stabilising System Frequency Using Hvdc between the Continental European, Nordic, and Great Britain Systems," *Sustainable Energy, Grids and Networks,* vol. 5, pp. 125-134, 3// 2016.
[11] Energynet.dk, "Energinet.Dk's Ancillary Services Strategy 2015-2017," 2015.
[12] Energynet.dk, "Energinet.Dk's Ancillary Services Strategy," 2011.
[13] J. Machowski, J. Bialek, and J. Bumby, *Power System Dynamics: Stability and Control*: WILEY, 2008.
[14] "Review of on-Line Dynamic Security Assessment Tools and Techniques," CIGRE Technical Brochure No. 325 2007.
[15] P. Kundur, *Power System Stability and Control*: McGraw-Hill Inc., 1994.
[16] A. Yazdani and R. Iravani, *Voltage-Sourced Converters in Power Systems : Modeling, Control, and Applications*: John Wiley & Sons, 2010.
[17] F. Golnaraghi and B. C. Kuo, *Automatic Control Systems*, 9th ed.: Wiley, 2009.
[18] P. M. Anderson, A. A. A. Fouad, I. o. Electrical, and E. Engineers, *Power System Control and Stability*: IEEE Press, 1993.